Scientific Research Publishing

Advances in Materials Physics and Chemistry, 2020, 10, 239-251
https://www.scirp.org/journal/ampc
ISSN Online: 2162-5328
ISSN Print: 2162-531X

Peierls Structural Transition in Q1D Organic Crystals of TTT_2I_3 for Different Values of Carrier Concentration

Silvia Andronic, Anatolie Casian

Department of Physics, Technical University of Moldova, Chisinau, Republic of Moldova
Email: silvia.andronic@mt.utm.md

How to cite this paper: Andronic, S. and Casian, A. (2020) Peierls Structural Transition in Q1D Organic Crystals of TTT_2I_3 for Different Values of Carrier Concentration. *Advances in Materials Physics and Chemistry*, **10**, 239-251.
https://doi.org/10.4236/ampc.2020.1010018

Received: July 20, 2020
Accepted: October 24, 2020
Published: October 27, 2020

Abstract

The Peierls structural transition in the TTT_2I_3 (tetrathiotetracene-iodide) crystal, for different values of carrier concentration is studied in 3D approximation. A crystal physical model is applied that considers two of the most important hole-phonon interactions. The first interaction describes the deformation potential and the second one is of polaron type. In the presented physical model, the interaction of carriers with the structural defects is taken into account. This is crucial for the explanation of the transition. The renormalized phonon spectrum is calculated in the random phase approximation for different temperatures applying the method of Green functions. The renormalized phonon frequencies for different temperatures are presented in two cases. In the first case the interaction between TTT chains is neglected. In the second one, this interaction is taken into account. Computer simulations for the 3D physical model of the TTT_2I_3 crystal are performed for different values of dimensionless Fermi momentum k_F, that is determined by variation of carrier concentration. It is shown that the transition is of Peierls type and strongly depends on iodine concentration. Finally, the Peierls critical temperature was determined.

Keywords

Quasi-One-Dimensional Organic Crystals, Peierls Structural Transition, TTT_2I_3, Renormalized Phonon Spectrum, Interchain Interaction, Peierls Critical Temperature

1. Introduction

During last year, organic materials have attracted increasing attention due to more diverse and unusual proprieties [1] [2] [3]. Recently, it was shown that

highly conducting Quasi-One-Dimensional (Q1D) organic crystals can have different promising thermoelectric applications [4] [5]. It was predicted in [6] that the values of dimensionless thermoelectric figure of merit ~4 could be realized after optimization of carrier concentration in TTT_2I_3 organic crystals. On the other hand, it is well known that organic nanomaterials have large potential applications in electronic, sensing, energy-harnessing and quantum-scale systems [7]. We mention that, the most studied organic crystals are those of tetrathiotetracene-iodide (TTT_2I_3) of *p*-type, tetrathiofulvalinium tetracyanoquinodimethane (TTF-TCNQ) of *n*-type and tetrathiotetracene tetracyanoquinodimethane ($TTT(TCNQ)_2$) of *n*-type. Q1D organic materials of TTT_2I_3, were synthesized independently [8] [9] [10] [11] with the aim to detect superconductivity in such a low-dimensional conductor. At the same time, these crystals show a metal-dielectric transition with decreasing temperature. Such transition has been observed in the Q1D charge transfer compound TTF-TCNQ in [12] [13]. This first experimental confirmation of the structural transition was predicted earlier by Rudolf Peierls [14] in 1D conductors. According to Peierls, for some lowered temperatures, the one-dimensional metallic crystal with a half filled conduction band has to pass in a dielectric state with a dimerized crystal lattice. This temperature T_p is called the Peierls critical temperature. Later, different authors [15]-[22] studied this phenomenon in different Q1D organic crystals. In TTF-TCNQ crystals, the metal-insulator transition takes place at 54 K into TCNQ stacks and at 38 K into TTF stacks. We recently studied the Peierls transition of TCNQ stacks [23]. The renormalized phonon spectrum was analyzed for different temperatures. We observed that with lowering temperature, some modifications in the phonon spectrum take place. For certain temperature, the renormalized phonon frequency becomes equal to zero for a given value of the phonon wave vector. We found that at 54 K the Peierls transition takes place.

The crystal of TTT_2I_3 is a charge transfer compound. The orthorhombic crystal structure consists of segregated chains or stacks of plane TTT molecules and of iodine chains. This compound is of mixed valence. Two molecules of TTT give one electron to iodine chain formed of I_3^- ions that play the role of acceptors. Only TTT chains are conductive and the carriers are holes. The electrons on iodine ions are in a rather localized states and do not participate in the transport. TTT_2I_3 crystal has the following lattice constants a = 18.40 Å, b = 4.96 Å and c = 18.32 Å, which demonstrates a very pronounced crystal quasi-one-dimensionality. The highly conducting direction is along $\boldsymbol{b}$. We investigated the Peierls transition in a 2D physical model for a $TTT_2I_{3.1}$ crystal [24]. In [25] the Peierls transition in the TTT_2I_3 crystals with the intermediate value of carrier concentration in 2D approximation was studied. It was applied a complete physical model [26], that considers two hole-phonon interaction mechanisms.

The conductivity properties of TTT stacks are very sensitive to defects and impurities [27]. This is caused by the purity of initial materials and the conditions of crystal growth. In TTT_2I_3 crystals, with the lowering of temperature the

conductivity firstly grows, reaches a maximum and after that falls. The temperature of the maximum, T_{max}, and the value of the ratio $\sigma_{max}/\sigma_{300}$ depends on the iodine content. Crystals with a surplus of iodine, $TTT_2I_{3.1}$, have T_{max} ~ (34 - 35) K and very sharp fall of $\sigma(T)$ (temperature dependence of electrical conductivity) after the maximum.

This paper reports on study of the Peierls transition in quasi-one-dimensional organic crystals TTT_2I_3. The main aim is to demonstrate that the sharp decrease of temperature dependence of electrical conductivity $\sigma(T)$ is determined by the structural transition in the TTT chains. Thus, we analyze the behavior of Peierls transition in organic crystals of TTT_2I_3 for different values of carrier concentration in 3D approximation. In the frame of the physical model we consider two hole-phonon interaction mechanisms. The first mechanism is of the deformation potential type and is determined by the variation of the transfer energy of a carrier from one molecule to the nearest one, caused by acoustic lattice vibrations. The second one is similar to that of polaron type, and it is determined by the variation of the polarization energy of molecules surrounding the conduction electron caused by the same acoustic vibrations. The dynamical interaction of carriers with the defects is also considered. We mention that, the Peierls structural transition in crystals of tetrathiotetracene-iodide, was not reported yet by other authors.

We start by analyzing the curves presented in **Figure 1** [27]. We show that the

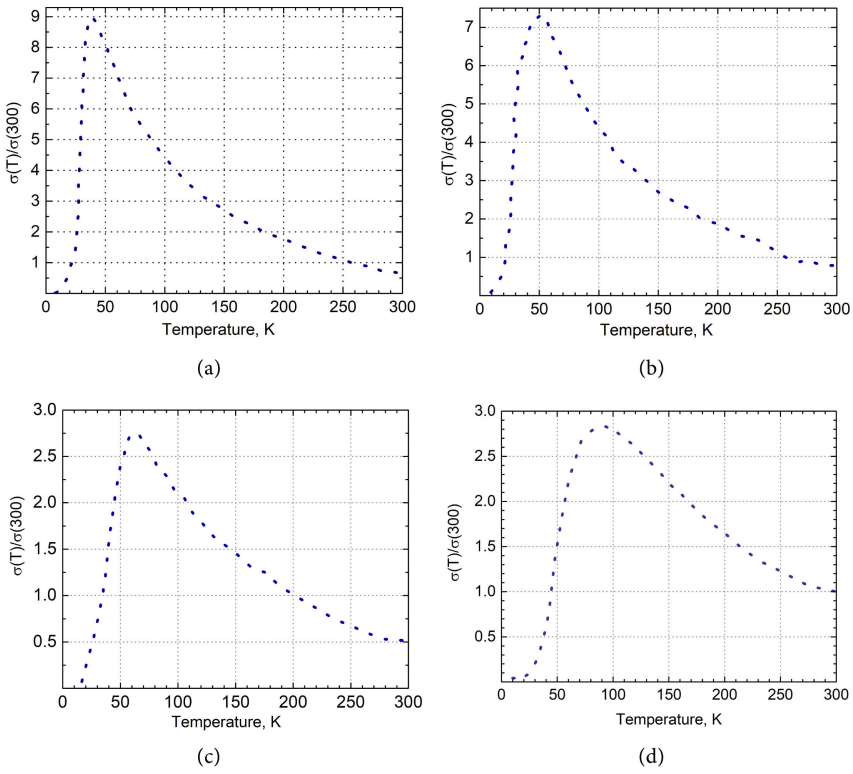

Figure 1. Temperature dependence of electrical conductivity of $TTT_2I_{3+\delta}$ crystal [27]. (a) δ = 0.1. Max-35 K, $\sigma \to 0$ at 10 K; (b) δ = 0.08. Max-50 K, $\sigma \to 0$ at 11 K; (c) δ = 0.06. Max-62 K, $\sigma \to 0$ at 12 K; (d) δ = 0.01. Max-90 K, $\sigma \to 0$ at 20 K.

Peierls structural transition explains the sharp decrease of electrical conductivity in TTT_2I_3 at low temperature. The Peierls critical temperature is determined. The paper is structured as follows. Section 2 describes three-dimensional model of the crystal. Section 3 presents the results of computer simulations. The conclusions are formulated in Section 4.

2. Three-Dimensional Physical Model of the Crystal

In this Section we will present the physical model of the TTT_2I_3 crystal that was described in more detail in [24]. The Hamiltonian of the 3D crystal model in the tight binding and nearest neighbor approximations is presented in the following form

$$H = \sum_{\boldsymbol{k}} \varepsilon(\boldsymbol{k}) a_{\boldsymbol{k}}^{+} a_{\boldsymbol{k}} + \sum_{\boldsymbol{q}} \hbar\omega_{\boldsymbol{q}} b_{\boldsymbol{q}}^{+} b_{\boldsymbol{q}} + \sum_{\boldsymbol{k},\boldsymbol{q}} A(\boldsymbol{k},\boldsymbol{q}) a_{\boldsymbol{k}}^{+} a_{\boldsymbol{k}+\boldsymbol{q}} \left(b_{\boldsymbol{q}} + b_{-\boldsymbol{q}}^{+}\right) \tag{1}$$

Let's analyze each term of Equation (1). The first term is the energy operator of free holes in the periodic field of the lattice. The second term represents the energy operator of longitudinal acoustic phonons. The third term describes the hole-phonon interactions. $\varepsilon(\boldsymbol{k})$ is the energy of the hole. By $a_{\boldsymbol{k}}^{+}, a_{\boldsymbol{k}}$ we denoted creation and annihilation operators of the hole with a 3D quasi-wave vector $\boldsymbol{k}$ and projections (k_x, k_y, k_z). $b_{\boldsymbol{q}}^{+}, b_{\boldsymbol{q}}$ are respectively the creation and annihilation operators of an acoustic phonon with 3D wave vector $\boldsymbol{q}$ and frequency ω_q. $A(\boldsymbol{k},\boldsymbol{q})$ is the matrix element of interaction. The energy of the hole $\varepsilon(\boldsymbol{k})$ is measured from the band top. This term is presented in the form

$$\varepsilon(\boldsymbol{k}) = -2w_1\left(1-\cos k_x b\right) - 2w_2\left(1-\cos k_y a\right) - 2w_3\left(1-\cos k_z c\right), \tag{2}$$

where w_1, w_2 and w_3 are the transfer energies of a hole from one molecule to another along the chain (x direction) and perpendicular to it (y and z directions), respectively.

It is well known, that the Peierls transition occurs at low temperatures. In this case, the interaction of electrons with optical phonons can be neglected. Thus, the spectrum of acoustic phonons of a simple one-dimensional chain can be described by [28]

$$\omega_{\boldsymbol{q}}^2 = \omega_1^2 \sin^2\left(q_x b/2\right) + \omega_2^2 \sin^2\left(q_y a/2\right) + \omega_3^2 \sin^2\left(q_z c/2\right), \tag{3}$$

where ω_1, ω_2 and ω_3 are the limit frequencies in the x, y and z directions, respectively. As was mentioned above, in the frame of this model we consider two hole-phonon interactions. The coupling constants of the first interaction are proportional to derivatives w_1', w_2' and w_3' with respect to the intermolecular distances. On the other hand, the coupling constant of the second interaction is proportional to the average polarizability of the molecule α_0. This interaction is important for crystals composed of large molecules, such as TTT, so as α_0 is roughly proportional to the molecule volume.

The square module of matrix element $A(\boldsymbol{k},\boldsymbol{q})$ of Hamiltonian (1) can be written in the form

$$\left|A(\boldsymbol{k},\boldsymbol{q})\right|^2 = 2\hbar w_1'^2 \Big/ \left(NM\omega_{\boldsymbol{q}}\right)\Big\{\Big[\sin\left(k_x b\right)-\sin\left(k_x-q_x,b\right)-\gamma_1\sin\left(q_x b\right)\Big]^2$$
$$+d_1^2\Big[\sin\left(k_y a\right)-\sin\left(k_y-q_y,a\right)-\gamma_2\sin\left(q_y a\right)\Big]^2 \quad (4)$$
$$+d_2^2\Big[\sin\left(k_z c\right)-\sin\left(k_z-q_z,c\right)-\gamma_3\sin\left(q_z c\right)\Big]^2\Big\}.$$

We notice that in Equation (4) several parameters are used for the detailed analysis of the crystal, considering the two hole-phonon interaction mechanisms mentioned above. Namely, M is the mass of the TTT molecule. N is the total number of molecules in the main region of the crystal. $d_1 = w_2/w_1 = w_2'/w_1'$; $d_2 = w_3/w_1 = w_3'/w_1'$. The parameters γ_1, γ_2 and γ_3 describe the ratio of amplitudes of the polaron-type interaction to the deformation potential one in the *x*, *y* and *z* directions, respectively. These parameters can be obtained from the following expressions

$$\gamma_1 = 2e^2\alpha_0/b^5 w_1', \quad \gamma_2 = 2e^2\alpha_0/a^5 w_2', \quad \gamma_3 = 2e^2\alpha_0/c^5 w_3' \quad (5)$$

To explain the behavior of the electrical conductivity from **Figure 1**, it is not sufficient to consider only hole-phonon interaction. It is necessary to take into account also the dynamical interaction of carriers with defects. The static interaction will give contribution to the renormalization of hole spectrum. The defects in TTT_2I_3 crystals are created due to different coefficients of dilatation of TTT iodine chains. The Hamiltonian of this interaction H_{def} is shown in the form

$$H_{\text{def}} = \sum_{\boldsymbol{k},\boldsymbol{q}}\sum_{n=1}^{N_d} B\left(q_x\right)\exp\left(-iq_x x_n\right)a_{\boldsymbol{k}}^{+}a_{\boldsymbol{k}-\boldsymbol{q}}\left(b_{\boldsymbol{q}}+b_{\boldsymbol{q}}^{-}\right). \quad (6)$$

In Equation (6), the term x_n numbers the defects, which are considered linear along *x*-direction of TTT chains, and distributed randomly. $B\left(q_x\right)$ is the matrix element of a hole interaction with a defect with the following form

$$B\left(q_x\right) = \sqrt{\hbar/\left(2NM\omega_q\right)}\cdot I\left(q_x\right). \quad (7)$$

Here $I\left(q_x\right)$ is the Fourier transformation of the derivative with respect to the intermolecular distance from the energy of interaction of a carrier with a defect

$$I\left(q_x\right) = D\left(\sin\left(bq_x\right)\right)^2, \quad (8)$$

where D is a parameter that determines the intensity of hole interaction with a defect and has the same meaning as w_1' in (5). The Peierls transition depends strongly on the value of this parameter.

The renormalized phonon spectrum $\Omega(\boldsymbol{q})$ is determined by the pole of the Green function obtained from the transcendent dispersion equation

$$\Omega(\boldsymbol{q}) = \omega_{\boldsymbol{q}}\left[1-\overline{\Pi}\left(\boldsymbol{q},\Omega\right)\right]^{1/2}, \quad (9)$$

where the principal value of the dimensionless polarization operator has the form

$$\mathrm{Re}\,\bar{\Pi}(\boldsymbol{q},\Omega)=-\frac{4}{\hbar\omega_q}\sum_{\boldsymbol{k}}\frac{\left[\left|A(\boldsymbol{k},-\boldsymbol{q})\right|^2+\left|B(q_x)\right|^2\right]\left(n_k-n_{k+q}\right)}{\varepsilon(\boldsymbol{k})-\varepsilon(\boldsymbol{k}+\boldsymbol{q})+\hbar\Omega}. \tag{10}$$

n_k is the Fermi distribution function. Finally, we mention that Equation (9) can be solved only numerically.

3. Results and Discussions

In the subsequent analysis, we perform the computer simulations for the 3D physical model of the crystal. The following set of parameters are used [29] $M = 6.5 \times 10^5 m_e$ (m_e is the mass of the free electron), $w_1 = 0.26$ eV·Å^{-1}, $d_1 = 0.015$, $\gamma_1 = 1.7$. γ_2 and γ_3 are determined from the relations $\gamma_2 = \gamma_1 b^5/a^5 d_1$ and $\gamma_3 = \gamma_1 b^5/c^5 d_2$. The sound velocity along TTT chains was estimated by comparison of the calculated results for the electrical conductivity of TTT_2I_3 crystals [29] with the reported ones in [10], $v_{s1} = 1.5 \times 10^5$ cm/s. For v_{s2} and v_{s3} in transversal directions (in the a direction and the c direction), we consider 1.35×10^5 cm/s and 1.3×10^5 cm/s, respectively. The numerical simulations are performed for different values of k_F, determined by variations in the carrier concentration. The parameter D which describes the intensity of a hole with a defect, varies in each case.

Figures 2-9 present the dependences for initial phonon frequency $\omega(q_x)$ and the dependences of renormalized phonon frequencies $\Omega(q_x)$ as a function of q_x for different temperatures and different values of q_y and q_z. As can be seen from figures, with a decrease of temperature T, the dependences change their form and a minimum appears. This minimum becomes more pronounced at lower temperatures. Also, it is seen that the values of $\Omega(q_x)$ are diminished in comparison with those of $\omega(q_x)$ in the absence of hole-phonon interaction. This means that the hole-phonon interaction and structural defects diminish the values of lattice elastic constants. In what follow we analyze the Peierls structural transition for the curves presented in **Figure 1**.

Figure 2 and **Figure 3** describe the behavior of the Peierls transition in TTT_2I_3 crystals with the higher value of carrier concentration. **Figure 2** shows the

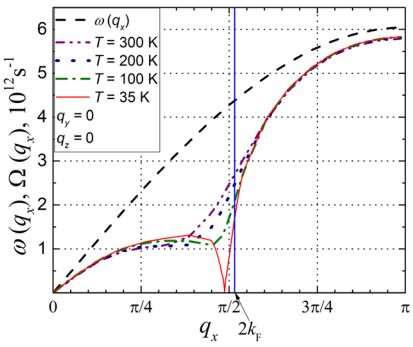

Figure 2. Renormalized phonon spectrum $\Omega(q_x)$ for $\gamma_1 = 1.7$ and different temperatures. The dashed line corresponds to the spectrum of free phonons. $k_F = 0.517 \cdot \pi/2$, $D = 1.036$ eV·Å^{-1}. Other parameters: $q_y = 0$, $q_z = 0$.

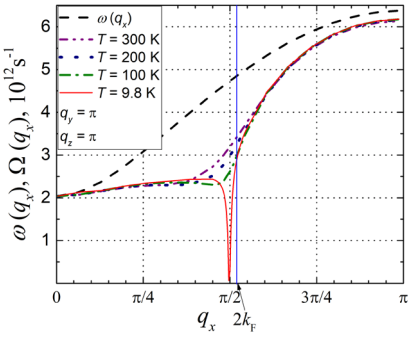

Figure 3. The same as in **Figure 2** for $k_F = 0.517 \cdot \pi/2$ and $D = 1.033$ eV·Å^{-1}. Other parameters: $q_y = \pi$, $q_z = \pi$.

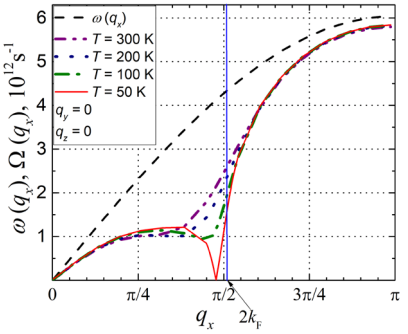

Figure 4. The same as in **Figure 2** for $k_F = 0.512 \cdot \pi/2$ and $D = 1.042$ eV·Å^{-1}. Other parameters: $q_y = 0$, $q_z = 0$.

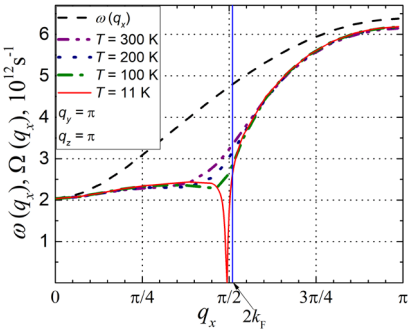

Figure 5. The same as in **Figure 2** for $k_F = 0.512 \cdot \pi/2$ and $D = 1.026$ eV·Å^{-1}. Other parameters: $q_y = \pi$, $q_z = \pi$.

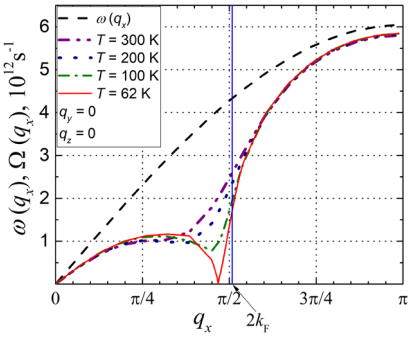

Figure 6. The same as in **Figure 2** for $k_F = 0.508 \cdot \pi/2$ and $D = 1.045$ eV·Å^{-1}. Other parameters: $q_y = 0$, $q_z = 0$.

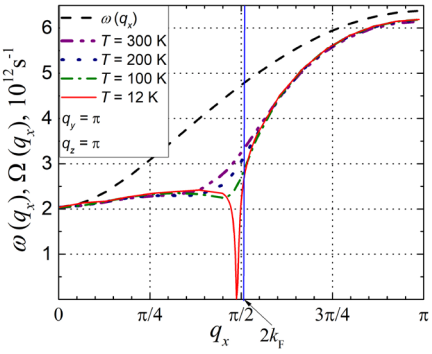

Figure 7. The same as in **Figure 2** for $k_F = 0.508 \cdot \pi/2$ and $D = 1.026$ eV·Å^{-1}. Other parameters: $q_y = \pi$, $q_z = \pi$.

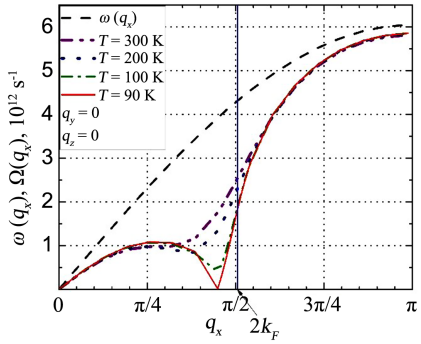

Figure 8. The same as in **Figure 2** for $k_F = 0.502 \cdot \pi/2$ and $D = 1.057$ eV·Å^{-1}. Other parameters: $q_y = 0$, $q_z = 0$.

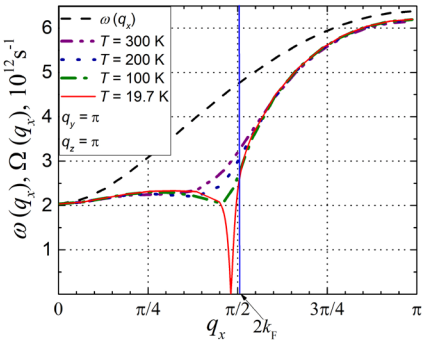

Figure 9. The same as in **Figure 2** for $k_F = 0.502 \cdot \pi/2$ and $D = 1.055$ eV·Å^{-1}. Other parameters: $q_y = \pi$, $q_z = \pi$.

renormalized phonon spectrum $\Omega(q_x)$ as a function of q_x, when $q_y = 0$ and $q_z = 0$ (the interaction between TTT chains is neglected). The dimensionless Fermi momentum $k_F = 0.517 \cdot \pi/2$. Parameter D ($D = 1.036$ eV·Å^{-1}) determines the intensity of hole interaction with a defect. The Peierls transition begins at $T = 35$ K. At this temperature, the electrical conductivity is strongly diminished (for comparison see **Figure 1(a)**), so as a gap in the carrier spectrum is fully opened just above the Fermi level.

If the interaction between transversal chains is taken into account ($q_y \neq 0$ and $q_z \neq 0$), the temperature at $\Omega(q_x) = 0$ is diminished. **Figure 3** shows the case

when $q_y = \pi$ and $q_z = \pi$, $k_F = 0.517 \cdot \pi/2$ and $D = 1.033$ eV·Å^{-1}. It was observed that parameter D decreases, or the hole interaction with a defect is smaller in this case. Analyzing the figure, one can see that the transition is completed at $T = 9.8$ K.

According to [27], the electrical conductivity significantly decreases and achieves zero at $T \sim 10$ K. Thus, our calculations show that the transition is of Peierls type and takes place at this temperature.

In Figures 4-7 we show the behavior of Peierls structural transition in organic crystals of TTT_2I_3 for intermediate values of carrier concentration. Figure 4 shows the case where the Fermi momentum decreases and has a value of $k_F = 0.512 \cdot \pi/2$. The interaction between TTT chains is neglected. Parameter D has a value of $D = 1.042$ eV·Å^{-1}. From the figure it is evident that the Peierls transition begins at $T = 50$ K. When the interaction between TTT chains is taken into account ($q_y = \pi$ and $q_z = \pi$), the temperature decreases considerably and the transition is completed at $T = 11$ K (see Figure 5). Now, the hole interaction with a defect is smaller $D = 1.026$ eV·Å^{-1}.

Figure 6 shows the case when the carrier concentration additionally decreases and $k_F = 0.508 \cdot \pi/2$. The Peierls transition begins at $T = 62$ K and is finished at $T = 12$ K (see Figure 7). Parameter D has a value $D = 1.045$ eV·Å^{-1}, when $q_y = 0$ and $q_z = 0$, and decreases to $D = 1.026$ eV·Å^{-1}, when $q_y = \pi$ and $q_z = \pi$.

Figure 8 and Figure 9 describe the Peierls transition in TTT_2I_3 crystals for the lowest value of carrier concentration. Figure 8 describes the case when $q_y = 0$ and $q_z = 0$ and the dimensionless Fermi momentum $k_F = 0.502 \cdot \pi/2$. Parameter D has a value of $D = 1.057$ eV·Å^{-1}. The interaction between TTT chains is neglected. In this case the Peierls transition begins at $T = 90$ K. At this temperature, the electrical conductivity achieves a maximum. With the lowering temperature, the electrical conductivity decreases. Figure 9 shows the case where the interaction between TTT chains is taken into account ($q_y = \pi$ and $q_z = \pi$), $D = 1.055$ eV·Å^{-1} and $k_F = 0.502 \cdot \pi/2$. As is observed from the figure, the transition is completed at $T = 19.7$ K. It is evident from Figure 1(d) that the electrical conductivity significantly decreases and achieves zero at $T \sim 20$ K. Also, it is observed that the parameter D decreases, or the hole interaction with a defect is smaller in this case.

The Peierls structural transition in Q1D organic crystals of TTT_2I_3, strongly depends on iodine concentration. From figures presented above and from Table 1 it was observed that with a decrease of the carrier concentration, the Peierls critical temperature increases.

4. Conclusion

The Peierls structural transition in Q1D organic crystal of TTT_2I_3 for different values of carrier concentration was studied in 3D approximation. In the frame of the crystal model, two of the most important hole-phonon interaction mechanisms are considered: of the deformation potential type and of the polaron type.

Table 1. The data presented in Figures 2-9.

Figure number	γ_1	k_F	q_y	q_z	D	Transition temperature
Figure 2	1.7	0.517·π/2	0	0	1.036	35 K
Figure 3	1.7	0.517·π/2	π,	π	1.033	9.8 K
Figure 4	1.7	0.512·π/2	0	0	1.042	50 K
Figure 5	1.7	0.512·π/2	π	π	1.026	11 K
Figure 6	1.7	0.508·π/2	0,	0	1.045	62 K
Figure 7	1.7	0.508·π/2	π	π	1.026	12 K
Figure 8	1.7	0.502·π/2	0,	0	1.057	90 K
Figure 9	1.7	0.502·π/2	π	π	1.055	19.7 K

The interaction of holes with the structural defects in direction of TTT chains was taken into account too. The renormalized phonon spectrum has been calculated in the random phase approximation. Computer simulations for renormalized phonon spectrum, $\Omega(q_x)$, for different temperatures are presented in two cases: 1) when the interaction between TTT chains is neglected ($q_y = 0$, $q_z = 0$) and 2) when the interaction between TTT chains is taken into account ($q_y = \pi$, $q_z = \pi$).

It was observed that the interchain interaction, reduces the transition temperature. The hole-phonon interaction and the interactions with structural defects diminish $\Omega(q_x)$ and reduce the sound velocity in a wide temperature range. When the interaction between TTT chains is taken into account, the parameter D decreases, or the hole interaction with a defect is smaller in this case. It was shown that the Peierls transition temperature strongly depends on iodine concentration. In this paper we analysed the dependences of the renormalized phonon spectrum for the following values of the carrier concentration.

1) When $k_F = 0.517 \cdot \pi/2$ and the hole concentration achieves the higher value in TTT_2I_3 crystal, the Peierls transition begins at $T \sim 35$ K in TTT chains and considerably reduces the electrical conductivity. Due to interchain interaction, the transition is completed at $T \sim 10$ K.

2) When the carrier concentration achieves an intermediate value, for $k_F = 0.512 \cdot \pi/2$, the Peierls transition begins at $T \sim 50$ K in TTT chains and is finished at $T \sim 11$ K.

3) When $k_F = 0.508 \cdot \pi/2$, the transition begins at $T \sim 62$ K in TTT chains and is completed at $T \sim 12$ K.

4) For the lowest values of hole concentration, when $k_F = 0.502 \cdot \pi/2$, the Peierls transition begins at $T \sim 90$ K in TTT chains. The electrical conductivity is considerably reduced. Due to interchain interaction, the transition is completed at $T \sim 20$ K.

Analyzing the behavior of the Peierls transition in the cases presented above, it can be observed that, with a decrease of the carrier concentration, the Peierls

critical temperature increases.

Acknowledgements

The authors express gratitude to the support from the scientific program under the project 20.80009.5007.08 and to V. Tronciu for useful comments.

Conflicts of Interest

The authors declare no conflicts of interest regarding the publication of this paper.

References

[1] Jerome, D. (2012) Organic Superconductors: When Correlations and Magnetism Walk In. *Journal of Superconductivity and Novel Magnetism*, **25**, 633-655. https://doi.org/10.1007/s10948-012-1475-7

[2] Pouget, J.P. (2012) Bond and Charge Ordering in Low-Dimensional Organic Conductors. *Physica B: Condensed Matter*, **407**, 1762-1770. https://doi.org/10.1016/j.physb.2012.01.025

[3] Sun, X., Zhang, L., Di, C., Wen, Y., Guo, Y., Zhao, Y., Yu, G. and Liu, Y. (2011) Morphology Optimization for the Fabrication of High Mobility Thin-Film Transistors. *Advanced Materials*, **23**, 3128-3133. https://doi.org/10.1002/adma.201101178

[4] Casian, A., Pflaum, J. and Sanduleac, I. (2015) Prospects of Low Dimensional Organic Materials for Thermoelectric Applications. *Journal of Thermoelectricity*, **1**, 16.

[5] Harada, K., Sumino, M., Adachi, C., Tanaka, S. and Miyazaki, K. (2010) Improved Thermoelectric Performance of Organic Thin-Film Elements Utilizing a Bilayer Structure of Pentacene and 2,3,5,6-Tetrafluoro-7,7,8,8-tetracyanoquinodimethane (F4-TCNQ). *Applied Physics Letters*, **96**, Article ID: 253304. https://doi.org/10.1063/1.3456394

[6] Casian, A. and Sanduleac, I. (2015) Thermoelectric Properties of Nanostructured Tetrathiotetracene Iodide Crystals: 3D Modeling. *Materials Today*: *Proceedings*, **2**, 504-509. https://doi.org/10.1016/j.matpr.2015.05.069

[7] Torres, T. and Bottari, G. (2013) Organic Nanomaterials: Synthesis, Characterization, and Device Applications. Wiley J. Sons Inc., Hoboken, 1-32.

[8] Buravov, I.I., Zvereva, G.I., Kaminskii, V.F., *et al.* (1976) New Organic "Metals": Naphthaceno[5,6-cd:11,12-c'd']bis[1,2]dithiolium Iodides. *Journal of the Chemical Society*, *Chemical Communications*, No. 18, 720-721. https://doi.org/10.1039/C39760000720

[9] Kaminskii, V.F., Khidekel, M.L., Lyubovskii, R.B., *et al.* (1977) Metal-Insulator Phase Transition in TTT_2I_3 Affected by Iodine Concentration. *Physica Status Solidi A*, **44**, 77-82. https://doi.org/10.1002/pssa.2210440107

[10] Hilti, B. and Mayer, C.W. (1978) Electrical Properties of the Organic Metallic Compound Bis(Tetrathiotetracene)-Triiodide, $(TTT)_2$-I_3. *Helvetica Chimica Acta*, **61**, 501-511. https://doi.org/10.1002/hlca.19780610143

[11] Isset, L.G. and Perz-Albuerene, E.A. (1977) Low Temperature Metallic Conductivity in Bis(Tetrathiotetracene) Triiodide, a New Organic Metal. *Solid State Communications*, **21**, 433-435. https://doi.org/10.1016/0038-1098(77)91368-0

[12] Ferraris, J., Cowan, D.O., Walatka, W. and Perlstein, J.H. (1973) Electron Transfer

in a New Highly Conducting Donor-Acceptor Complex. *Journal of the American Chemical Society*, **95**, 948-949. https://doi.org/10.1021/ja00784a066

[13] Coleman, L.B., Cohen, M.J., Sandman, D.J., Yamagishi, F.G., Garito, A.F. and Heeger, A.J. (1973) Superconducting Fluctuations and the Peierls Instability in an Organic Solid. *Solid State Communications*, **12**, 1125-1132. https://doi.org/10.1016/0038-1098(73)90127-0

[14] Peierls, R. (1955) Quantum Theory of Solids. Oxford University Press, London, 433-435.

[15] Bulaevskii, L.N. (1975) Peierls Structure Transition in Quasi-One-Dimensional Crystals. *Soviet Physics Uspekhi*, **18**, 131. https://doi.org/10.1070/PU1975v018n02ABEH001950

[16] Khanna, S.K., Pouget, J.P., Comes, R., Garito, A.F. and Heeger, A.J. (1977) X-Ray Studies of $2k_F$ and $4k_F$ Anomalies in Tetrathiafulvalene-Tetracyanoquinodimethane (TTF-TCNQ). *Physical Review B*, **16**, 1468. https://doi.org/10.1103/PhysRevB.16.1468

[17] Jerome, D. (2004) Organic Conductors: From Charge Density Wave TTF-TCNQ to Superconducting $(TMTSF)_2PF_6$. *Chemical Reviews*, **104**, 5565-5592. https://doi.org/10.1021/cr030652g

[18] Jerome, D. and Schulz, H.J. (1982) Organic Conductors and Superconductors. *Advances in Physics*, **31**, 299-490. https://doi.org/10.1080/00018738200101398

[19] Pouget, J.P. (1988) Highly Conducting Quasi-One-Dimensional Organic Crystals, Semiconductors and Semimetals. Chapter 3, Vol. 27, Academic Press, New York, 87-214.

[20] Pouget, J.P. (2016) The Peierls Instability and Charge Density Wave in One-Dimensional Electronic Conductors. *Comptes Rendus Physique*, **17**, 332-356. https://doi.org/10.1016/j.crhy.2015.11.008

[21] Chernenkaya, A., *et al.* (2015) Nature of the Empty States and Signature of the Charge Density Wave Instability and Upper Peierls Transition of TTF-TCNQ by Temperature-Dependent NEXAFS Spectroscopy. *The European Physical Journal B*, **88**, 13. https://doi.org/10.1140/epjb/e2014-50481-9

[22] Streltsov, S.V. and Khomskii, D.I. (2014) Orbital-Dependent Singlet Dimers and Orbital-Selective Peierls Transitions in Transition-Metal Compounds. *Physical Review B*, **89**, Article ID: 161112. https://doi.org/10.1103/PhysRevB.89.161112

[23] Andronic, S. and Casian, A. (2016) Phonons near Peierls Structural Transition in Quasi-One-Dimensional in Organic Crystals of TTF-TCNQ. *Advances in Materials Physics and Chemistry*, **6**, 98-104. https://doi.org/10.4236/ampc.2016.64010

[24] Andronic, S. and Casian, A. (2017) Metal-Insulator Transition of Peierls Type in Quasi-One-Dimensional Crystals of TTT_2I_3. *Advances in Materials Physics and Chemistry*, **7**, 212-222. https://doi.org/10.4236/ampc.2017.75017

[25] Andronic, S., Sanduleac, I. and Casian, A. (2020) Peierls Structural Transition in Organic Crystals of TTT_2I_3 with Intermediate Carrier Concentration. In: 4*th International Conference on Nanotechnologies and Biomedical Engineering*, Springer, Berlin, 199-202. https://doi.org/10.1007/978-3-030-31866-6_40

[26] Casian, A., Dusciac, V. and Coropceanu, Iu. (2002) Huge Carrier Mobilities Expected in Quasi-One-Dimensional Organic Crystals. *Physical Review B*, **66**, Article ID: 165404. https://doi.org/10.1103/PhysRevB.66.165404

[27] Shchegolev, I.F. and Yagubskii, E.B. (1982) Extended Linear Chain Compounds. Plenum Press, New York, Vol. 2, 385. https://doi.org/10.1007/978-1-4684-3932-8_9

[28] Graja, A. (1989) Low-Dimensional Organic Conductors. Word Scientific, Singapore.

[29] Casian, A. and Sanduleac, I. (2014) Thermoelectric Properties of Tetrathiotetracene Iodide Crystals: Modeling and Experiment. *Journal of Electronic Materials*, **43**, 3740-3745. https://doi.org/10.1007/s11664-014-3105-6